# The Effects of Seat Racks and Buffer Materials on Floating Packaging Parts Swing and Overturning Safety

Dapeng Zhu, Chenghu Wu

Abstract—Two measures, namely using a support frame and cushioning materials, are employed to improve the sway-overturn safety of the floating packaging. The packaging is placed on the support frame, with viscoelastic bearings installed beneath the frame. A two-degree-of-freedom motion equation for the packaging and support frame under impact excitation is developed, and a numerical analysis method for the sway motion of the packaging and the horizontal motion of the support frame is established. Dimensional analysis is used to study the factors affecting the sway-overturn safety of the packaging. To further improve the sway-overturn safety of the packaging, cushioning materials are applied to the support frame. A three-degree-of-freedom motion equation for the support frame and packaging under impact excitation is constructed, and a numerical analysis method for the support frame's sway, vertical, and horizontal motion is established. The analysis results show that the excitation waveform influences the effectiveness of the support frame. Under half-sine excitation, the support frame is beneficial to safety improvement. Under full-sine excitation, when  $\omega_c/p$  is large, the support frame improves safety. In contrast, when  $\omega / p$  is low, the support frame decreases safety. Reducing the elastic coefficient of the bearings is beneficial for improving safety. Under half-sine excitation, increasing the bearing damping coefficient reduces safety. When  $\omega p$  is high, cushioning materials are highly effective in improving safety.

*Index Terms*—floating packaging, sway-overturn safety, support frame, cushioning materials

#### I. INTRODUCTION

ENSURING packaging safety during transport under various load conditions is a core issue in transportation packaging. Researchers mainly focus on packaging safety under drop impact and random vibration loads [1-3]. The findings are of significant theoretical value for improving packaging transportation safety, enhancing packaging design, and improving packaging testing methods. In engineering

Manuscript received January 27, 2025; revised August 17, 2025.

This work was supported by the National Natural Science Foundation of China (Grant No. 12162020) and the Gansu Provincial Key Research and Development Project (Grant No. 25YFGA048).

Dapeng Zhu is a professor in the School of Transportation, Lanzhou Jiaotong University, Lanzhou, Gansu 730070, PR China (Corresponding author to provide e-mail: zhudapeng@mail.lzjtu.cn).

Chenghu Wu is a postgraduate student in the School of Transportation, Lanzhou Jiaotong University, Lanzhou, Gansu 730070, PR China (e-mail: 878563741@qq.com).

practice, many large goods or packaging, such as large electromechanical products and prefabricated building components, cannot be effectively reinforced due to constraints such as loading efficiency, labor costs, and reinforcement conditions. These packaging must be floated during transport on vehicles or containers. During transport, under the influence of vibration and shock loads, these floating packages will sway, and if the swaying angle exceeds a certain limit, the packaging will overturn. The overturning of packaging causes damage to goods and often leads to vehicle damage, traffic accidents, and other serious consequences. Therefore, studying the sway phenomenon of floating packaging during transportation is of significant practical importance for packaging transportation safety.

Research on the sway problem of floating packaging in transportation packaging is still limited. The sway of floating packaging during transport can be modeled as the swaying problem of a rigid mass block under bearing excitation. This problem has attracted significant attention in earthquake engineering and cultural heritage preservation fields. Housner GW [4] proposed modeling buildings as rigid mass blocks and established the inverted pendulum motion equation for the swaying of mass blocks. References [5-8] have proposed dynamic response analysis methods for rigid mass blocks under various shock loads and established overturning boundary curves for rigid mass blocks, providing the basis for the sway-overturn safety analysis of packaging. Charalampakis A E et al. [9] comprehensively considered the forced and free responses of rigid mass blocks under shock loads and constructed the overturning conditions for rigid mass blocks under shock excitation. Although the swaying of rigid mass blocks is structurally simple, it belongs to a piecewise smooth nonlinear system with collisions, exhibiting rich dynamic characteristics under certain conditions. References [10,11] explored various dynamic characteristics of rigid mass block swaying and analyzed the conditions under which various dynamic phenomena occur, focusing on the dynamic phenomena affecting the overturning of mass blocks. Due to the negative stiffness characteristics of swaying structures and their self-resetting ability, using appropriate swaying structures in bridges and buildings can improve the seismic resistance of systems [12,13]. The swaying response of rigid mass blocks is often difficult to analyze directly. Brzeski Pet al. [14] used the Runge-Kutta method to analyze the swaying of rigid mass blocks. However, this method has the disadvantages of low analytical efficiency and high computational costs. Sieber Met al. [15] used numerical analysis methods to analyze the correlation between the maximum swaying angle of rigid mass blocks, overturning risks, and seismic load indicators. The analysis showed that using the peak velocity of the load could effectively predict the maximum swaying angle of the rigid mass block. To efficiently analyze the swaying response and overturning risk of rigid mass blocks, references [16-18] used neural networks, machine learning, and other methods to construct models for the swaying response of rigid mass blocks. Although these models require a large amount of simulation or experimental data during the training process, once established, these intelligent models can quickly predict the maximum swaying angle of the rigid mass block, whether it will overturn, etc. These models can also reveal the key factors affecting rigid mass blocks' swaying characteristics.

During the transportation of large packaging, to avoid heavy load concentration and improve transportation safety, the packaging is usually placed on a support frame, and both the packaging and the support frame are placed in a vehicle or container for transport. This paper uses two commonly used engineering vibration reduction measures to reduce the swaying response of floating packaging during transportation and decrease the overturning risk of packaging: (1) Installing viscoelastic bearings between the support frame and the vehicle. Under the longitudinal load of the vehicle, the bearing undergoes longitudinal deformation, absorbing part of the load energy and reducing the packaging's response; (2) Laying cushioning materials on the support frame, which absorb part of the energy during the packaging's motion, reducing the packaging's response. To study the effect of these two measures on the sway-overturn safety of packaging, this paper constructs a response analysis method for floating packaging support under shock loads. It investigates the effect of viscoelastic bearings and cushioning materials on the sway safety of packaging. It analyzes the impact of the support frame, bearing, and cushioning characteristics on packaging sway safety. The research in this paper provides important theoretical guidance for designing cushioning measures for floating packaging and improving transportation safety.

## II. THE DYNAMIC CHARACTERISTICS OF STAND AND FLOATING PACKAGING PARTS

To improve transportation safety, the floating packaging is placed on a support frame for transport, with viscoelastic bearings installed between the support frame and the vehicle, as shown in Fig. 1. It is assumed that there is no relative sliding between the packaging and the support frame, and that after a collision between the packaging and the support frame during the swaying process, no rebound occurs. Under the longitudinal acceleration  $\ddot{u}_{_g}$  of the vehicle, the packaging and support frame may exhibit two types of motion modes: (1) simultaneous lateral movement, and (2) the packaging sways on the laterally moving support frame. The motion of the support frame and the packaging can be described using the variables u and  $\theta$ , where u is the displacement of the support frame relative to the vehicle,  $\theta$  is the swaying angle of the packaging, as shown in Fig. 1. It is assumed that the packaging is homogeneous and symmetric, with a height of

2h, a width of 2b,  $R = \sqrt{h^2 + b^2}$  and a mass of m. The rotational inertia of the packaging about its center of mass point C is  $I_C$ , and  $\tan \alpha = b/h$ . The mass of the support frame is  $m_b$ . When the support frame moves to the right, it is assumed that u > 0, and when the packaging rotates clockwise,  $\theta > 0$ . Under the influence of  $\ddot{u}_g$ , the packaging will not sway when

the condition  $|\ddot{u}_g + \ddot{u}| < gb/h$  is met. The acceleration due to gravity is g = 9.8 m/s<sup>2</sup>. The motion equations for the packaging and the support frame are as follows:

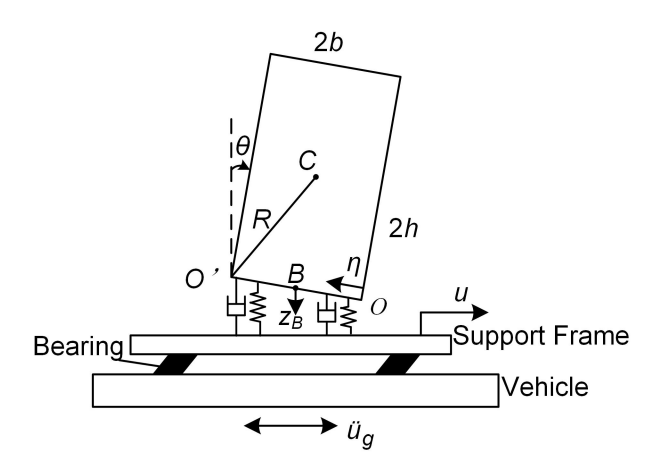


Fig.1 .Model for the motion of package and rigid pedestal.

$$(m + m_b)(\ddot{u}_g + \ddot{u}) + k_b u + c_b \dot{u} = 0$$
 (1)

Where  $k_b$  and  $c_b$  are the equivalent elastic coefficient and damping coefficient of the bearing, respectively. Define the

param 
$$\omega_b = \sqrt{\frac{k_b}{m + m_b}}$$
, and  $\zeta_b = \frac{c_b}{2\omega_b(m + m_b)}$ , then Equation

(1) simplifies to:

$$\ddot{u} + 2\zeta_b \omega_b \dot{u} + \omega_b^2 u = -\ddot{u}_g \tag{2}$$

When  $|\ddot{u}_g + \ddot{u}| \ge gb/h$  is reached, the packaging swells on the moving support frame. Considering the force balance and torque balance in the horizontal direction, and applying D'Alembert's principle, the motion equations for the packaging and the support frame are constructed as follows:

$$(m+m_b)(\ddot{u}+\ddot{u}_g)+k_bu+c_b\dot{u}$$

$$+ mR\cos(\alpha - \operatorname{sgn}(\theta)\theta)\ddot{\theta} + mR\sin(\operatorname{sgn}(\theta)\alpha - \theta)\dot{\theta}^2 = 0$$
(3)

$$(I_C + mR^2)\ddot{\theta} + mR\cos(\alpha - \operatorname{sgn}(\theta)\theta)(\ddot{u} + \ddot{u}_g) + mgR\sin(\operatorname{sgn}(\theta)\alpha - \theta) = 0$$
(4)

Define the parameters 
$$p = \sqrt{\frac{3g}{4R}}$$
 and  $\gamma = \frac{m}{m + m_b}$ . Then,

Equations (3) and (4) can be simplified as follows:

$$\ddot{u} = \frac{-2\zeta_b \omega_b \dot{u} - \omega_b^2 u + p^2 \gamma R \cos A_1 \sin A_2 - \gamma R \sin A_2 \dot{\theta}^2}{1 - p^2 \gamma R \cos^2 A_1 / g} - \ddot{u}_g$$
(5)

$$\ddot{\theta} = \frac{p^2 \cos A_1 / g \left( 2\zeta_b \omega_b \dot{u} + \omega_b^2 u + p^2 \gamma R \sin A_2 \dot{\theta}^2 \right) - p^2 \sin A_2}{1 - p^2 \gamma R \cos^2 A_1 / g}$$

Where:  $A_1 = \alpha - \text{sgn}(\theta)\theta$ ,  $A_2 = \text{sgn}(\theta)\alpha - \theta$ . To analyze the motion of the packaging and the support frame using the

Runge-Kutta method, the state vector is constructed as follows: A, with T representing the transpose of the vector. Taking the derivative of the state vector y(t) gives:

$$\dot{\mathbf{y}}(t) = \begin{bmatrix} \dot{u}(t) & \dot{\theta}(t) & \ddot{u}(t) & \ddot{\theta}(t) \end{bmatrix}^T \tag{7}$$

Equations (5) to (7) represent the coupled differential equations for u and  $\theta$ , which can be solved using the classical Runge-Kutta method.

When the packaging sways on the support frame, at  $\theta=0$ , the packaging and the support frame collide. Due to the conservation of the instantaneous angular momentum of the packaging about point O before and after the collision, the following can be obtained:

$$I_O\dot{\theta}^- - 2mRb\sin\alpha\dot{\theta}^- + mh\dot{u}^- = I_O\dot{\theta}^+ + mh\dot{u}^+ \tag{8}$$

The superscripts - and + represent the instantaneous values before and after the collision, respectively.  $I_O$  is the rotational inertia of the packaging about point O or point O'. Additionally, considering the conservation of linear momentum before and after the collision between the packaging and the support frame, the following can be obtained:

$$(m+m_b)\dot{u}^- + mh\dot{\theta}^- = (m+m_b)\dot{u}^+ + mh\dot{\theta}^+$$
 (9)

By combining Equations (5) and (6), the relationship between the changes in the motion states of the packaging and the support frame before and after the collision can be obtained:

$$\dot{\theta}^{+} = \frac{(\gamma + 4)\cot^{2}\alpha - 2(\gamma + 1)}{(\gamma + 4)\cot^{2}\alpha + 4(\gamma + 1)}\dot{\theta}^{-}$$
 (10)

$$\dot{u}^{+} = \dot{u}^{-} + \frac{6\gamma h}{(\gamma + 4)\cot^{2}\alpha + 4(\gamma + 1)}\dot{\theta}^{-}$$
 (11)

## III. THE DYNAMIC CHARACTERISTICS OF THE SEAT AND FLOATING PACKAGING PART OF THE BUFFER MATERIAL

In engineering practice, cushioning materials can be laid on the support frame to further improve the safety of the floating packaging. An accurate model of the cushioning material must be constructed to study the impact of the cushioning material on the safety of the packaging. Commonly used models include the Winkler model [19,20], the Hunt-Crossley nonlinear collision model [21], and the Hertz contact model [22]. In this study, the Winkler model is used to analyze the effect of cushioning material properties on the safety of the floating packaging. The Winkler model represents the cushioning material laid on the support frame as a continuously distributed linear spring and damper, as shown in Fig. 2. After the longitudinal load  $\ddot{u}_g$  from the vehicle is applied to the support frame, the packaging placed on the cushioning material will exhibit swaying motion and vertical motion relative to the support frame. It is assumed that the vertical displacement of the midpoint B at the bottom of the packaging is  $z_B$ . When point B moves downward,  $z_B > 0$ . Applying D'Alembert's principle and considering the vertical force and torque balance at point B, the following relationship can be obtained:

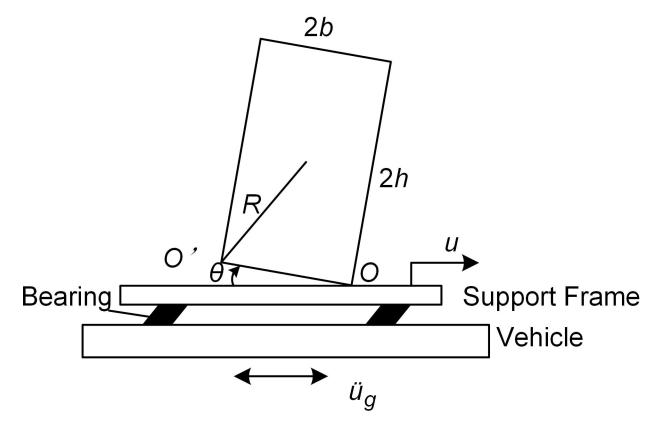


Fig.2. Model for the motion of package and pedestal paved with cushion material.

$$m\ddot{z}_B + mh(\dot{\theta}^2\cos\theta + \ddot{\theta}\sin\theta) + F_B - mg = 0$$
 (12)

$$(I_C + mh^2)\ddot{\theta} + mh\ddot{u}_b \cos\theta + mh(\ddot{z}_B - g)\sin\theta + M_B + mh\ddot{u}_a \cos\theta = 0$$
(13)

Here,  $F_B$  and  $M_B$  represent the concentrated contact force and torque exerted by the cushioning material on the packaging at point B during the interaction between the cushioning material and the packaging. Additionally, the motion equations of the packaging and the support frame relative to the vehicle are determined by Equation (3). Using the Winkler model to characterize the properties of the cushioning material, the vertical contact force F between the packaging and the cushioning material can be expressed as follows:

$$F(\eta, t) = kz(\eta, t) + c\dot{z}(\eta, t) \tag{14}$$

Here, k and c represent the elasticity and damping properties of the cushioning material, respectively.  $\eta$  is the distance from the bottom of the packaging to point O, and  $z(\eta,t)$  is the vertical displacement of the bottom of the packaging at time t, at a distance  $\eta$  from point O. According to Fig. 2, in Equation (14), the displacement and velocity at any point on the bottom of the packaging can be expressed as follows:

$$z(\eta, t) = z_O - \eta \sin \theta \tag{15}$$

$$\dot{z}(\eta, t) = \dot{z}_0 - \eta \dot{\theta} \cos \theta \tag{16}$$

Here,  $z_O$  and  $\dot{z}_O$  represent the vertical displacement and velocity at point O:  $z_O = z_B + b sin\theta$ . When the packaging sways on top of the cushioning material, if  $\theta$  is small, the bottom of the packaging and the cushioning material are in full contact. When  $\theta$  is large, part of the bottom of the packaging and the cushioning material will lose contact. In these two cases, the contact force  $F_B$  and contact torque  $M_B$  generated during the interaction between the packaging and the cushioning material can be expressed as follows:

When  $z_B > b \sin|\theta|$ , the bottom of the packaging is in full contact with the cushioning material, as shown in Fig. 3, then:

$$F_{B} = \int_{0}^{2b} F(\eta, t) d\eta = 2b (kz_{B} + c\dot{z}_{B})$$
 (17)

$$M_{B} = \int_{0}^{2b} F(\eta, t)(b - \eta) \cos \theta d\eta$$
$$= \frac{2}{3} b^{3} \cos \theta \left( k \sin \theta + c \dot{\theta} \cos \theta \right)$$
(18)

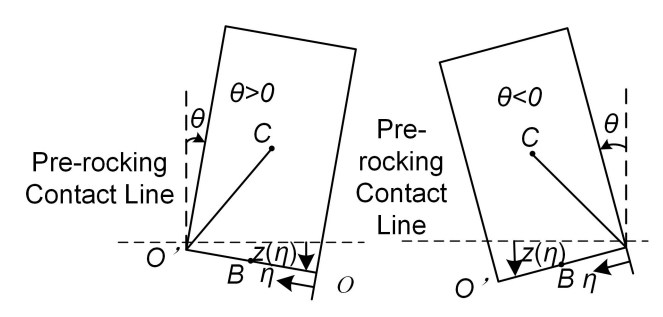


Fig.3. Condition of full contact of package with cushion material.

When  $z_B < b \sin |\theta|$ , the bottom of the packaging makes partial contact with the cushioning material, as shown in Fig. 4, then:

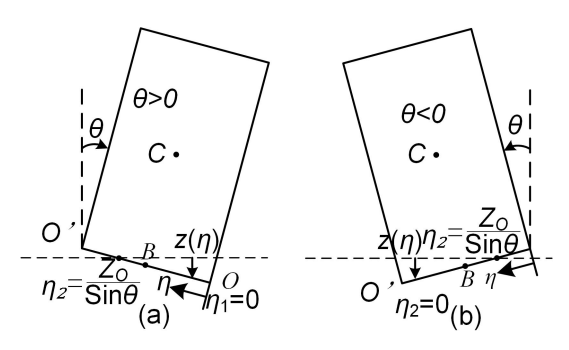


Fig.4. The packaging and the cushioning material are in partial contact.

$$F_{B} = \int_{\eta_{1}}^{\eta_{2}} F(\eta, t) d\eta = \frac{1}{2} b^{2} k \sin \theta \operatorname{sgn} \theta + k z_{B} \left( b + \frac{1}{2} \frac{z_{B}}{\sin \theta} \operatorname{sgn} \theta \right) + c \dot{z}_{B} \left( b + \frac{z_{B}}{\sin \theta} \operatorname{sgn} \theta \right)$$
(19)
$$+ \frac{1}{2} c \dot{\theta} \cos \theta \left( b^{2} - \frac{1}{2} \frac{z_{B}^{2}}{\sin^{2} \theta} \right) \operatorname{sgn} \theta$$
(19)
$$M_{B} = \int_{\eta_{1}}^{\eta_{2}} F(\eta, t) (b - \eta) \cos \theta d\eta = \frac{1}{3} b^{3} k \cos \theta \sin \theta$$

$$+ \frac{1}{2} k z_{B} \cos \theta \left( b^{2} - \frac{1}{3} \frac{z_{B}^{2}}{\sin^{2} \theta} \right) \operatorname{sgn} \theta$$

$$+ \frac{1}{2} c \dot{z}_{B} \cos \theta \left( b^{2} - \frac{z_{B}^{2}}{\sin^{2} \theta} \right) \operatorname{sgn} \theta$$

$$+ \frac{1}{3} c \dot{\theta} \cos^{2} \theta \left( b^{3} + \frac{z_{B}^{3}}{\sin^{3} \theta} \operatorname{sgn} \theta \right)$$
(20)

The integration limits  $\eta_1$  and  $\eta_2$  differ when  $\theta > 0$  and  $\theta < 0$ , and their expressions are listed in Fig. 4.

By combining Equations (3), (12), and (13), the following can be obtained:

$$\Omega \ddot{\theta} = p^2 \begin{pmatrix} -M_B + R\cos\alpha \\ \left( F_B \sin\theta + m\cos\theta \left( \Phi + R\dot{\theta}^2 \cos\alpha\sin\theta \right) \right) \end{pmatrix}$$
 (21)

$$\ddot{u} = -\Phi - (R\gamma \cos A_1)\ddot{\theta} - \ddot{u}_g \tag{22}$$

$$\ddot{z}_{B} = -h(\dot{\theta}^{2}\cos\theta + \ddot{\theta}\sin\theta) + \frac{F_{B}}{m} + g$$
 (23)

Among them:

$$\Omega = mR \left( g - p^2 R \left( \sin^2 \alpha - \gamma \cos \alpha \cos \theta \cos A_1 - \cos^2 \alpha \sin^2 \theta \right) \right)$$
 (24)

$$\Phi = 2\zeta\omega u + \omega^2 u + R\gamma\sin A_2\dot{\theta}^2 \tag{25}$$

Construct the motion state vector for the support frame with the cushioning material laid on it and the packaging

$$\mathbf{Y}(t) = \begin{bmatrix} u(t) & \theta(t) & z_B(t) & \dot{u}(t) & \dot{\theta}(t) & \dot{z}_B(t) \end{bmatrix}^T.$$
Taking the derivative of the state vector  $\mathbf{Y}(t)$  gives:

$$\dot{\mathbf{Y}}(t) = \begin{bmatrix} \dot{u}(t) & \dot{\theta}(t) & \dot{z}_{\scriptscriptstyle B}(t) & \ddot{u}(t) & \ddot{\theta}(t) & \ddot{z}_{\scriptscriptstyle B}(t) \end{bmatrix}^T \tag{26}$$

According to Equations (21) to (26), the Runge-Kutta method can be used to analyze the motion responses u(t),  $\theta(t)$ , and  $z_B(t)$  of the packaging and the support frame with cushioning material.

During the collision process, the system's kinetic energy and potential energy satisfy:

$$\frac{1}{2}I_0\dot{\theta}^2 + \frac{1}{2}(m+m_b)\dot{u}^2 = mgh(1-\cos\theta) + \frac{1}{2}k_bu^2$$
 (27)

Here,  $I_O$  is the moment of inertia of the packaging about the pivot point O, and h is the height of the center of mass.

When considering the nonlinear properties of the cushioning material, Equation (14) is modified as follows:

$$F(\eta,t) = kz(\eta,t) + c\dot{z}(\eta,t) + \beta z(\eta,t)^{3}$$
 (28)

It is recommended that footnotes be avoided (except for the unnumbered footnote with the receipt date on the first page). Instead, integrate the footnote information into the text and the reference part.

## IV. THE EFFECTS OF RACKS ON FLOATING PACKAGING PARTS AND SWAYING AND OVERTURNING SAFETY

First, without considering the cushioning material, the impact of the support frame characteristics on the packaging's sway and overturning safety is studied. The packaging is placed on the support frame, and under the vehicle's acceleration load  $\ddot{u}_{s}$ , the responses of the packaging and the support frame are divided into two stages:

- (1) At point  $|\ddot{u}_g + \ddot{u}| < gb/h$ , the packaging and the support frame move together in thehorizontally. According to Equation (2), the Runge-Kutta method analyzes the packaging and the support frame's horizontal displacement response u(t).
- (2) At point  $|\ddot{u}_g + \ddot{u}| > gb/h$ , the packaging begins to sway on the support frame. Based on Equations (5) to (11), and considering the velocity and displacement of the support frame when the packaging starts to sway, the Runge-Kutta method is used to analyze the sway response  $\theta(t)$  of the packaging and the horizontal displacement response u(t) of the support frame.

Assuming the amplitude of the vehicle excitation is  $a_e$ , and the frequency is  $\omega_e$ , according to Equations (5) and (6), during the motion of the support frame and packaging, their responses u(t) and  $\theta(t)$  are functions of eight variables, namely:

$$u(t) = f_1(p, \alpha, g, \omega_b, \zeta_b, \gamma, a_e, \omega_e)$$
 (29)

$$\theta(t) = f_2(p, \alpha, g, \omega_b, \zeta_b, \gamma, a_e, \omega_e)$$
 (30)

Due to the many factors affecting the packaging's sway response, to analyze the main factors influencing the sway response, the variables in Equations (26) and (29) are expressed in terms of length L, time T, and angle  $\Theta$ . The dimensional representation of each variable is as follows:  $[\theta] = \Theta$ , [u] = L,  $[p] = T^{-1}$ ,  $[\alpha] = \Theta$ ,  $[g] = LT^{-2}$ ,  $[\omega_b] = T^{-1}$ ,  $[\zeta_b]$  is dimensionless,  $[\gamma]$  is dimensionless,  $[a_e] = LT^{-2}$ ,  $[\omega_b] = T^{-1}$ . According to the  $\Pi$  theorem proposed by Buckingham [23] and by analyzing the dimensional homogeneity and balance [23,24], the responses u(t) and  $\theta(t)$  are determined by the following eight dimensionless parameters [25]:

$$\Pi_{1} = \frac{u\omega_{e}^{2}}{a_{e}}, \Pi_{2} = \theta, \Pi_{3} = \frac{\omega_{b}}{\omega_{e}}, \Pi_{4} = \zeta,$$

$$\Pi_{5} = \gamma, \Pi_{6} = \frac{\omega_{e}}{p}, \Pi_{7} = \tan\alpha, \Pi_{8} = \frac{a_{e}}{g}$$
(31)

Based on the results of the dimensional analysis and Equation (31), by using  $\Pi6$  as the horizontal coordinate and  $\Pi8/\Pi7$  as the vertical coordinate, the boundary curve for packaging overturning under different  $\Pi3$  conditions can be analyzed. Taking half-sine and full-sine impact excitations as examples, the packaging responses are analyzed using the Runge-Kutta method according to Equations (5) to (11). The basic parameters of the packaging and the support frame are shown in Table I , and the packaging sway overturning boundary curve is shown in Fig. 5.

TABLE I PARAMETERS VALUE IN THE EXAMPLE

Parameter	m	R	γ	α	$\omega_b/\omega_e$	$\omega_e$	$\zeta_b$
Value	1 (t)	0.5~2.0 (m)	0. 8	20 (°)	1、1/2、 1/3	5~30 (rad/s)	0.1

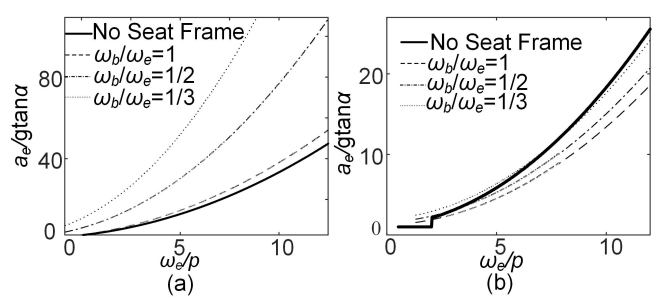


Fig. 5. Packaging sway overturning boundary curve placed on the support frame: (a) half-sine excitation, (b) full-sine excitation.

Fig. 5(a) shows that the support frame can effectively increase the packaging's overturning boundary under half-sine excitation. The softer the support frame beneath (smaller  $\omega_b/\omega_e$ ), the better the packaging's resistance to overturning. Under full-sine excitation, without the use of the support frame, the packaging exhibits two overturning modes: when  $\omega_e/p$  is small, the packaging overturns after one collision with the support frame; when  $\omega_e/p$  is large, the packaging starts swaying and then directly overturns. After installing the support frame, under full-sine impact excitation, the packaging only exhibits one overturning mode: the packaging starts to sway on the support frame and then directly overturns. When  $\omega_e/p$  is small (i.e., when the vibration excitation period is extended or the packaging size is small), installing the support frame improves the packaging's sway overturning safety. When  $\omega_e/p$  is large (i.e., when the vibration excitation period is short or the packaging size is large), installing the support frame decreases the packaging's sway overturning safety. A softer support frame

(smaller  $\omega_b/\omega_e$ ) is improves the packaging's sway ,overturning safety.

By changing the parameter  $\gamma$  in Table I while keeping other parameters constant, the effect of different  $\gamma$  values on the packaging's sway overturning boundary is analyzed. The results are shown in Fig. 6. From Fig. 6; it can be seen that increasing the support frame's mass  $m_b$  and reducing  $\gamma$  can effectively improve the packaging's sway overturning safety. This measure is effective under both half-sine and full-sine excitation conditions. Therefore, when cost permits, it is advisable to select a heavier support frame to improve the packaging's sway overturning safety.

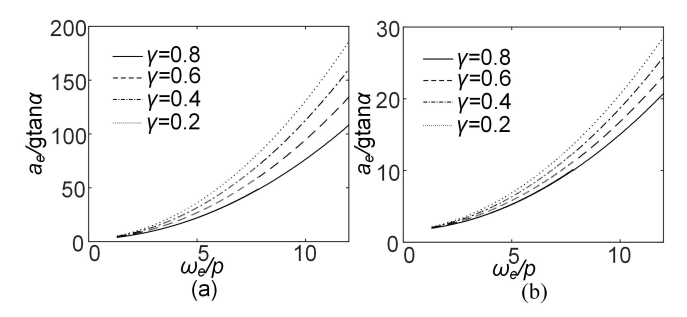


Fig. 6. Effect of γ on the packaging's sway overturning boundary: (a) half-sine excitation, (b) full-sine excitation.

By changing the parameter  $\zeta_b$  in Table I while keeping other parameters constant, the effect of different  $\zeta_b$  values on the packaging's sway overturning boundary is analyzed. The results are shown in Fig. 7. From Fig. 7, the effect of the support damping coefficient ζ b on the packaging's sway overturning safety varies under different impact excitation waveforms. Under full-sine excitation, increasing the support damping coefficient helps improve the packaging's sway overturning safety. However, increasing the support damping coefficient reduces the packaging's sway ,overturning safety under half-sine excitation. A heavier support frame (low y value) enhances safety but increases material costs and the vehicle's load burden. It is recommended that safety and economy be balanced through lightweight design (such as honeycomb aluminum structures). The stiffness adjustment of elastic supports should match the vehicle's chassis structure, and complex installations may reduce loading and unloading efficiency. Modular support frame designs can simplify on-site operations.

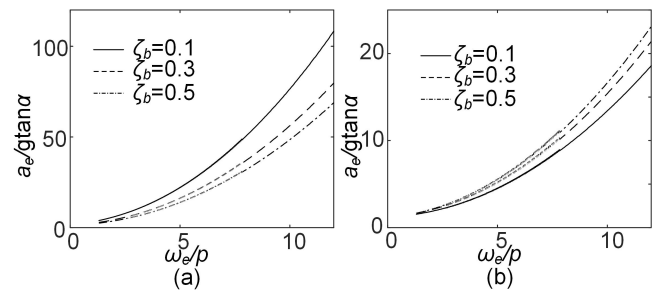


Fig. 7. Effect of  $\zeta_b$  on the packaging's sway overturning boundary: (a) half-sine excitation, (b) full-sine excitation.

V. THE IMPACT OF BUFFER MATERIALS ON THE SAFETY OF FLOATING PACKAGING PARTS AND SWAYING SAFETY

The packaging is placed on a support frame with

cushioning material, and under impact excitation; the packaging's response includes the following three stages:

- (1) During the initial stage of impact excitation, the horizontal response of the packaging and the support frame is small. When  $|\ddot{u}_g + \ddot{u}| < gb/h$  occurs, the packaging and the support frame move together horizontally. According to Equation (2), the Runge-Kutta method is used to analyze the horizontal response of the packaging.
- (2) At point  $|\ddot{u}_g + \ddot{u}| > gb/h$ , it swells while the packaging moves horizontally with the support frame. In the initial swaying stage, the sway response angle  $\theta$  is small. When  $z_B >$  b  $\sin |\theta|$ , the packaging and the cushioning material are in complete contact. The force  $F_B$  and torque  $M_B$  exerted by the cushioning material on the packaging are determined by Equations (17) and (18). Substituting these into Equations (21) to (23) and using Equation (26), along with the initial displacement and velocity of the packaging and the support frame when the packaging begins to sway, the Runge-Kutta method is used to analyze the response of the packaging and the support frame.
- (3) As the sway response angle  $\theta$  increases, when  $z_B < b \sin|\theta|$ , the packaging and the cushioning material are in partial contact. At this point, Equations (19) and (20) determine the force FB and torque  $M_B$ . Substituting these into Equations (21) to (23) and using Equation (26), along with the initial state of the packaging at this moment, the Runge-Kutta method is used to analyze the response of the packaging and the support frame.

Defining parameters  $\omega_c = \sqrt{k/m}$  and  $\zeta_c = c/2m\omega_c$ , the sway motion equation of the packaging on the support frame with cushioning material is constructed to analyze its sway motion. The basic parameters are shown in Table I. Under both half-sine and full-sine excitation, the sway overturning boundary curves of the packaging under different  $\omega_c$  and  $\zeta_c$  conditions are shown in Fig. 8 and Fig. 9.

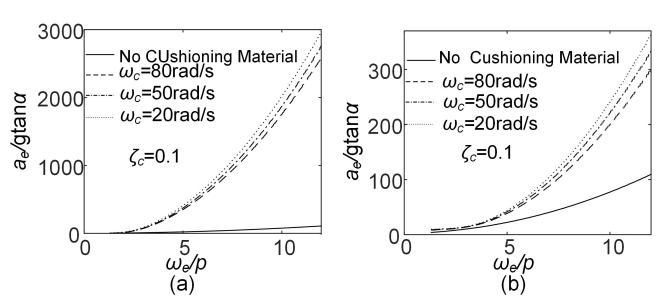


Fig. 8. Effect of  $\omega_c$  on the packaging's sway overturning boundary: (a) half-sine excitation, (b) full-sine excitation.

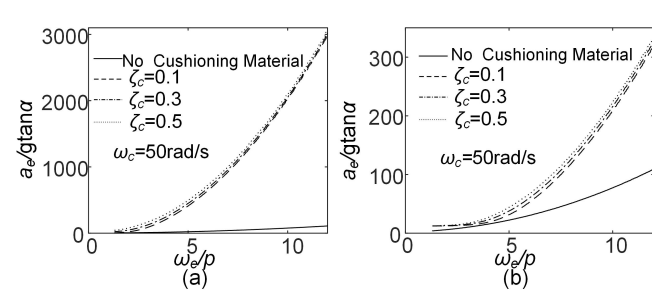


Fig. 9. Effect of  $\zeta_c$  on the packaging's sway overturning boundary: (a) half-sine excitation, (b) full-sine excitation.

Figs. 8 and 9 show that installing cushioning material with

certain elasticity and damping on the support frame can improve the packaging's sway overturning safety. When  $\omega p$  is small, meaning the load frequency is low, or the packaging size is large, the cushioning material has a more negligible effect on improving sway overturning safety. When  $\omega p$  is large, meaning the load frequency is high, or the packaging size is small, the cushioning material can significantly improve the sway overturning safety of the packaging. Comparing Fig. 8(a) and Fig. 8(b), under half-sine excitation, the effect of the cushioning material on packaging sway overturning safety is much higher than under full-sine excitation.

From Fig. 9, it can be seen that increasing the damping coefficient  $\zeta_c$  of the cushioning material can improve the packaging 's sway overturning safety. However, the improvement is limited, especially under half-sine excitation, where the damping coefficient  $\zeta_c$  has little impact on the packaging's sway overturning safety. Therefore, when laying cushioning material on the support frame, the elastic properties of the cushioning material should be given primary consideration. Additionally, the temperature and humidity sensitivity of the cushioning material (e.g., polyurethane aging) may affect long-term performance, so environmental durability testing should be included when selecting materials.

Based on the numerical analysis results, under full-sine excitation, if the support frame is not installed, the packaging may overturn in two modes: when  $\omega p$  is small, the packaging overturns after a reverse sway and collision with the vehicle, and when  $\omega p$  is large, the packaging directly overturns after swaying. After installing the support frame under full-sine excitation with different amplitudes and frequencies, due to the buffering effect of the support frame, the packaging 's sway motion will only exhibit one overturning mode: direct sway overturning. After laying cushioning material on the support frame, under full-sine excitation, the packaging may initially undergo reverse swaying; however, after colliding with the support frame during the reverse sway motion, the packaging will not overturn, and only one overturning mode will exist: direct overturning. Therefore, under full-sine excitation, the support frame can change the packaging's sway motion and overturning modes. After laying cushioning material on the support frame, the cushioning material can alter the packaging's sway motion mode, but it will not change the sway overturning mode.

#### VI. IN CONCLUSION

This paper proposes two measures to improve the sway overturning safety of floating packaging during transport: (1) placing the packaging on a support frame and installing viscoelastic supports at the bottom of the frame; (2) laying cushioning material on the surface of the support frame. The motion equations for the packaging and support frame are established to study the effect of the support frame on the packaging's sway overturning safety. The motion equations for the packaging and support frame with cushioning material are developed to examine the effect of the cushioning

material on the packaging's sway overturning safety. The main conclusions of this study are as follows:

- (1) Under different vehicle load conditions with varying waveforms, the impact of the support frame on the packaging's sway overturning safety differs. Under half-sine load conditions, installing the support frame helps improve the packaging's sway overturning safety. Under full-sine load conditions, the support frame changes the packaging's sway motion and overturning modes. When  $\omega_c/p$  is large, installing the support frame helps improve sway overturning safety. When  $\omega_c/p$  is small, installing the support frame reduces the sway overturning safety. Therefore, under full-sine excitation, when the excitation frequency is low ,or the packaging size is large, it is not advisable to transport floating packaging with the support frame. In this case, it is recommended that the floating packaging be reinforced to improve sway overturning safety.
- (2) The support under the support frame affects the sway overturning safety of the floating packaging. The softer the support, the higher the packaging's overturning safety. The damping coefficient of the support has an entirely different effect on sway overturning safety under different excitation waveforms. Under full-sine excitation, increasing the support's damping coefficient improves the packaging's sway-overturning safety, whereas under half-sine excitation, increasing the support damping reduces the packaging's sway-overturning safety.
- (3) Increasing the mass of the support frame (decreasing the coefficient  $\gamma$ ) helps improve the packaging 's sway overturning safety.
- (4) Laying cushioning material on the support frame helps improve the packaging 's sway, overturning safety. When  $\omega /p$  is large, laying cushioning material significantly improves the packaging 's sway overturning safety. When  $\omega /p$  is small, laying cushioning material still improves sway overturning safety but to a lesser extent. This indicates that if the impact load period is extended or the packaging size is large, laying cushioning material on the support frame has a limited effect on improving the packaging 's sway overturning safety.
- (5) Reducing the cushioning material's elasticity coefficient and increasing its damping coefficient both help improve the packaging's sway overturning safety, but the damping coefficient's effect on overturning safety is small.
- (6) The cushioning material on the support frame can change the packaging's sway motion mode but not alter its sway overturning mode.
- (7) Future research directions: ① Multi-physics coupling modeling: A more detailed multi-body dynamics model should be established considering the coupling effect of flexible deformation of internal cargo and external excitation. ② Intelligent control technology: Combining active damping systems (e.g., magnetorheological supports) with real-time feedback control to dynamically adjust support stiffness in response to complex road conditions. ③ Standardized design guidelines: Based on big data and machine learning, a packaging-support frame parameter database should be constructed to promote the development of industry design standards.

#### REFERENCE

- Huo, Y.-L., Ji, X.-L., Liu, Y.-H. (2021). MSLP Analytical Solution for Dropping Shock of Damped Hyperbolic Tangent Nonlinearity Packaging System. Packaging Engineering, 42(17), 168-173.
- [2] Yang, S. P., Wang, Z. W. (2021). Acceleration Spectrum Analysis of Hyperbolic Tangent Package Under Random Excitation. Packaging Technology and Science, 34(9), 579-587.
- [3] Zhu, D., Wang, H., Cao, X. (2023). Package Response Characteristics Analysis Under Non-Gaussian Loads. Journal of Vibration and Shock, 42(2), 100-107.
- [4] Housner, G. W. (1963). The Behavior of Inverted Pendulum Structures During Earthquakes. Bulletin of the Seismological Society of America, 53(2), 403-417.
- [5] Makris, N. (2014). A Half-Century of Rocking Isolation. Earthquakes and Structures, 7(6), 1187-1221.
- [6] Dimitrakopoulos, E. G., DeJong, M. J. (2012). Revisiting the Rocking Block: Closed-Form Solutions and Similarity Laws. Proceedings of the Royal Society A: Mathematical, Physical and Engineering Sciences, 468(2144), 2294-2318.
- [7] Voyagaki, E., Psycharis, I. N., Mylonakis, G. (2013). Rocking Response and Overturning Criteria for Free Standing Rigid Blocks to Single-Lobe Pulses. Soil Dynamics and Earthquake Engineering, 46, 85-95
- [8] Neto, J. P. J. (2017). Solving the Nonlinear Pendulum Equation with Nonhomogeneous Initial Conditions. International Journal of Applied Mathematics, 30(3), 259-266.
- [9] Charalampakis, A. E., Tsiatas, G. C., Tsopelas, P. (2022). New Insights on Rocking of Rigid Blocks: Analytical Solutions and Exact Energy-Based Overturning Criteria. Earthquake Engineering & Structural Dynamics, 51(9), 1965-1993.
- [10] Hogan, S. J. (1989). On the Dynamics of Rigid-Block Motion Under Harmonic Forcing. Proceedings of the Royal Society of London. A. Mathematical and Physical Sciences, 425(1869), 441-476.
- [11] Liu, Y., Páez Chávez, J., Brzeski, P., et al. (2021). Dynamical Response of a Rocking Rigid Block. Chaos: An Interdisciplinary Journal of Nonlinear Science, 31(7), 073136.
- [12] Zhou, W., Wang, X., Nie, L., et al. (2024). Seismic Performance Analysis of Self-Centering Rocking Pier of High-Speed Railway. China Railway Science, 45(3), 38-49.
- [13] Li, G., Zhang, W., Wang, Y., Sun, F. (2021). Seismic Response Characteristics of Dual-Stage Energy Dissipation Rocking Structure System. Journal of Vibration and Shock, 40(5), 92-101.
- [14] Brzeski, P., Kapitaniak, T., Perlikowski, P. (2016). The Use of Tuned Mass Absorber to Prevent Overturning of the Rigid Block During Earthquake. International Journal of Structural Stability and Dynamics, 16(10), 1550075.
- [15] Sieber, M., Vassiliou, M. F., Anastasopoulos, I. (2022). Intensity Measures, Fragility Analysis and Dimensionality Reduction of Rocking Under Far-Field Ground Motions. Earthquake Engineering & Structural Dynamics, 51(15), 3639-3657.
- [16] Zhu, D., Qi, Z., Cao, X. (2024). Research on Freestanding Package Nonlinear Rocking Response Under Vehicle Braking Condition. Journal of Vibration and Shock, 43(16), 152-158.
- [17] Banimahd, S. A., Giouvanidis, A. I., Karimzadeh, S., et al. (2024). A Multi-Level Approach to Predict the Seismic Response of Rigid Rocking Structures Using Artificial Neural Networks. Earthquake Engineering & Structural Dynamics, 53(6), 2185-2208.
- [18] Achmet, Z., Diamantopoulos, S., Fragiadakis, M. (2024). Rapid Seismic Response Prediction of Rocking Blocks Using Machine Learning. Bulletin of Earthquake Engineering, 22(7), 3471-3489.
- [19] Chatzis, M. N., Smyth, A. W. (2012). Robust Modeling of the Rocking Problem. Journal of Engineering Mechanics, 138(3), 247-262.
- [20] Spanos, P. D., Di Matteo, A., Pirrotta, A., et al. (2017). Rocking of Rigid Block on Nonlinear Flexible Foundation. International Journal of Non-Linear Mechanics. 94, 362-374.
- [21] Hunt, K. H., Crossley, F. R. E. (1975). Coefficient of Restitution Interpreted as Damping in Vibroimpact. Journal of Applied Mechanics, 42(2), 440-445.
- [22] Dintwa, E., Tijskens, E., Ramon, H. (2008). On the Accuracy of the Hertz Model to Describe the Normal Contact of Soft Elastic Spheres. Granular Matter, 10, 209-221.
- [23] Barenblatt, G. I. (1996). Scaling, Self-Similarity, and Intermediate Asymptotics: Dimensional Analysis and Intermediate Asymptotics. Cambridge University Press.
- [24] Dimitrakopoulos, E. G., DeJong, M. J. (2012). Revisiting the Rocking Block: Closed-Form Solutions and Similarity Laws. Proceedings of the

### **IAENG International Journal of Applied Mathematics**

- Royal Society A: Mathematical, Physical and Engineering Sciences, 468(2144), 2294-2318.
- Vassiliou, M. F., Makris, N. (2012). Analysis of the Rocking Response of Rigid Blocks Standing Free on a Seismically Isolated Base. Earthquake Engineering & Structural Dynamics, 41(2), 177-196